
4.1 Design of Solar Panel Tracking System

A newly developed solar tracking system is introduced with its adjustable orientation angle to track daily sunlight in 3D directions in order to receive the maximum solar energy via systematic photovoltaic arrays. The driving mechanisms designed with gear train unit in this solar tracking system can orientate solar system between east and west and a rotating table can orientate solar unit between north and south. The prototype of this new solar tracking system is depicted in Figs. 4.1 and 4.2.

Figure 4.1 shows the prototype of this new solar tracking system that has an orientation rack and orientation base (with stepper motor and gear reducer inside) installed to rotate solar panel frame in the eastern-western direction and has motor driving system, base plate, and orientation plate mounted to keep solar panel frame gradually rotating to follow sun's yearly travel in north-south orbit. Several detecting sensors are installed to trace the sunlight through receiving varied current signals from photodiodes in order to automatically manipulate the solar panel rotation in eastern-western and northern-southern 3D directions.

4.2 Computer-Aided Simulation of Solar Panel Tracking System

This new solar tracking system is designed based on analysis of computer-aided modeling and numerical simulation. The 3D modeling of the solar tracking system is performed by 3D CAD software and structure analysis is carried out by FEA technique. The structure analysis includes validating the functionality and strength of driving system in east-west and north-south solar panel orientation.

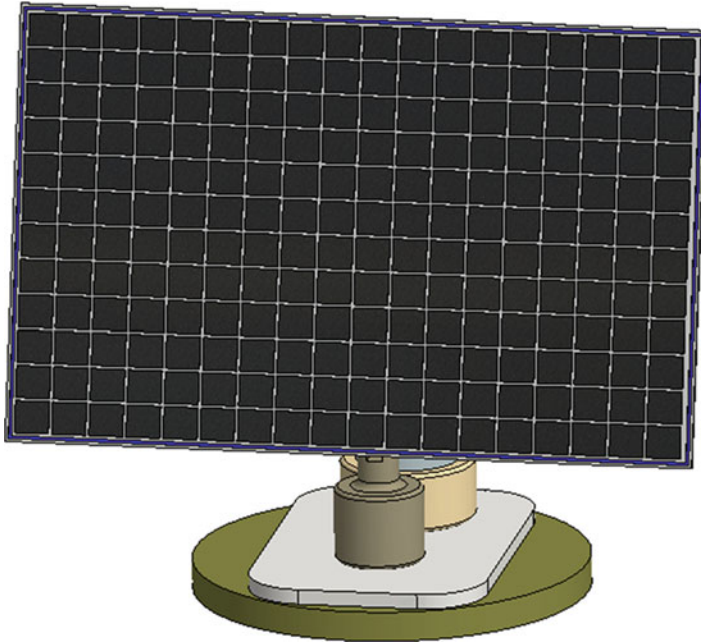


Fig. 4.1 Solar panel system front view

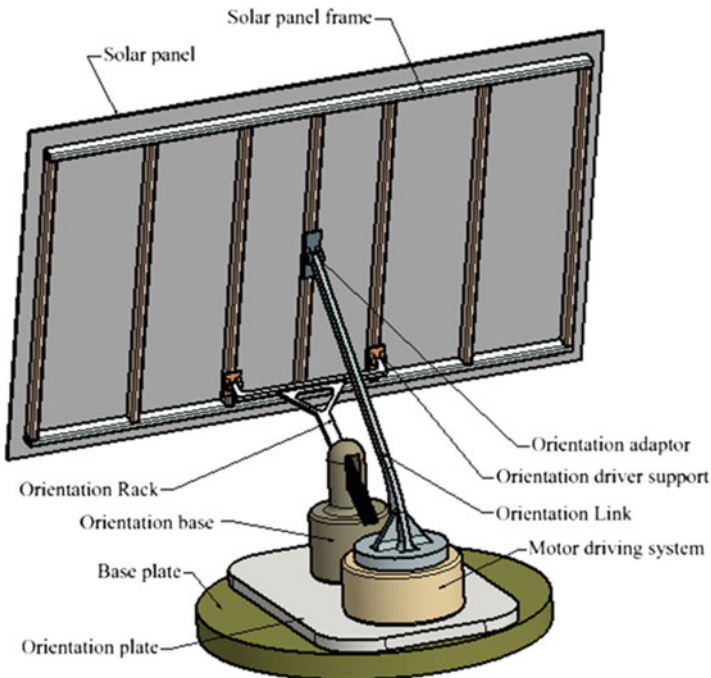


Fig. 4.2 Solar panel system rear view

1. Calculation of wind force:

The wind load required should be considered in the solar tracking system design to make sure that all the functioning parts, such as panel frame, lateral channel beam, longitudinal channel beam, orientation adaptor, orientation rack, orientation base, orientation driver support, and orientation link, will still work under the maximum wind load in worst conditions. The wind load equation can be expressed as follows (Mehta and Coulburne 2010):

$$F_{\text{wind}} = A_{\text{project}} \times P_{\text{wind}} \times D_{\text{drag}} \quad (4.1)$$

The wind pressure P_{wind} can be defined by the following equation:

$$P_{\text{wind}} = 0.00256 \times V_{\text{wind}}^2 \quad (4.2)$$

Here, F_{wind} —load caused by wind (lbf), A_{project} —projected surface area of solar panel at different orientation (ft^2), P_{wind} —pressure caused by wind (psf), D_{drag} —coefficient of drag, and V_{wind} —speed of wind (mph).

2. Calculation of gear-train force in solar panel orientation:

To keep the gears from damage during solar panel tracking system operation, the gear train must be able to handle the resultant force from force of wind, weight of solar panel and hardware, and other related frictional forces. The resultant force can be determined as follows (Mehta and Coulburne 2010):

$$\begin{aligned} T_{\text{panel}}(\text{torque to orientate the solar panel}) &= N_d \times 0.5 \times d_p \\ &= F_R \times 0.5 \times D_{\text{gear}} \end{aligned} \quad (4.3)$$

$$F_R = W_{\text{total weight}} \times C_f$$

Here, N_d —force to drive gear (N), d —gear pitch diameter, F_R —orientation force (N), D_O —outside gear diameter, W_{TW} —total weight of solar panel system (kg), and C_f —friction coefficient of different contact materials. The force to drive gears changes when solar panel orientates to the different angles which can be determined through computer-aided modeling and simulation.

Figures 4.3, 4.4, 4.5, 4.6, 4.7, 4.8, 4.9, 4.10, 4.11, 4.12, 4.13, 4.14, 4.15, 4.16, 4.17, 4.18, 4.19, 4.20, 4.21, 4.22, 4.23, 4.24, 4.25, 4.26, 4.27, 4.28, and 4.29 show the 3D part models, stress profile, and deflection profile of critical components in this new solar tracking system.

The computer-aided simulation and analysis in Figs. 4.4 and 4.5 demonstrate the stress and deflection profiles of newly designed solar panel system. The analytic results present that the maximum stress of 2,267.076 psi in this solar panel system is less than the material yield strength of 36,300 psi and maximum deflection of 0.00507 in. is within material allowable deformation limit.

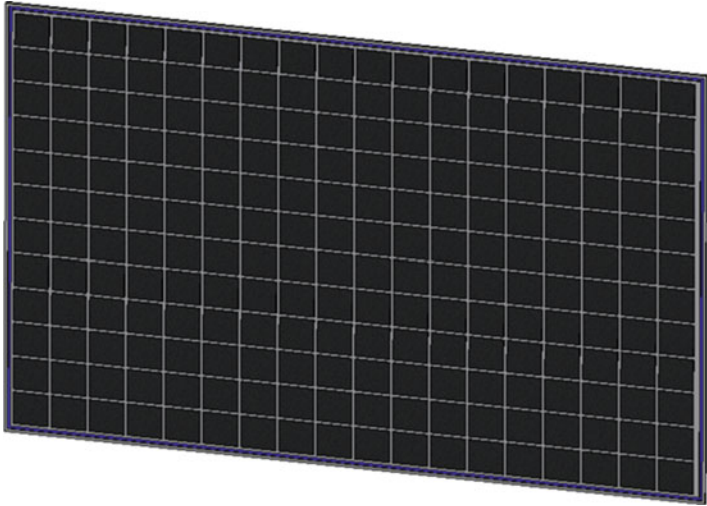


Fig. 4.3 Solar panel

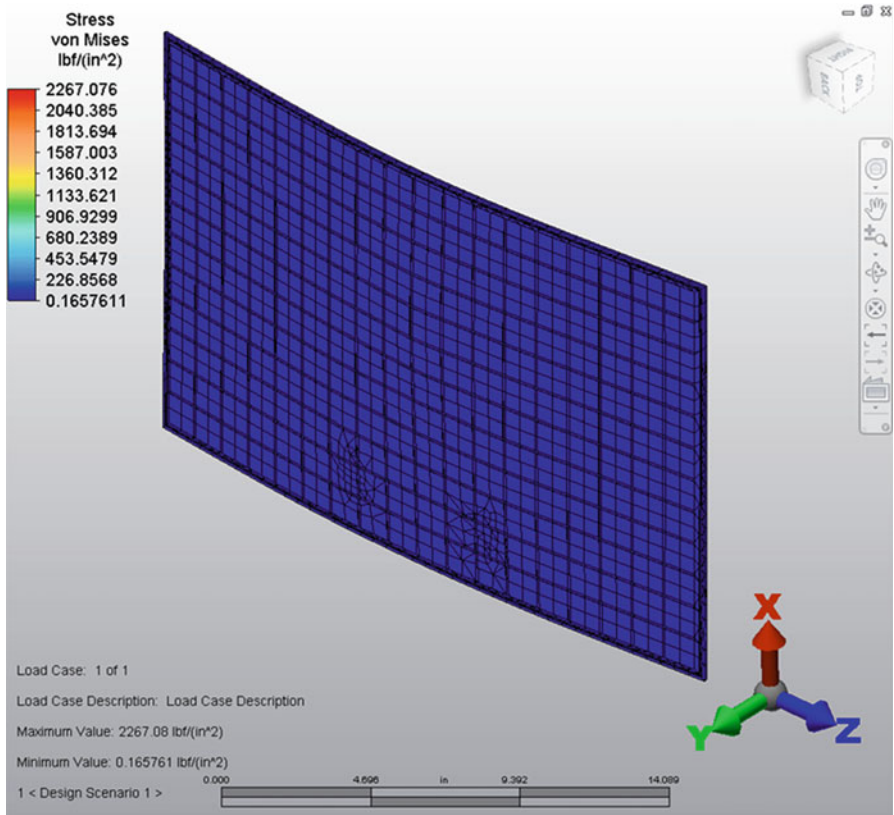


Fig. 4.4 Stress profile in solar panel

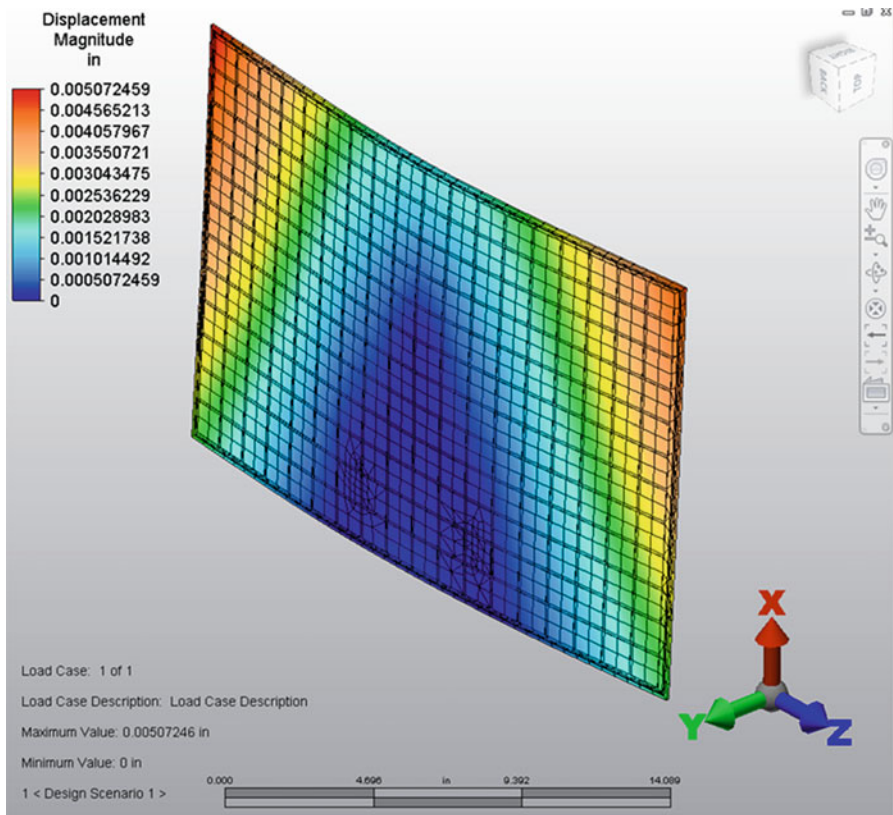


Fig. 4.5 Deflection profile in solar panel

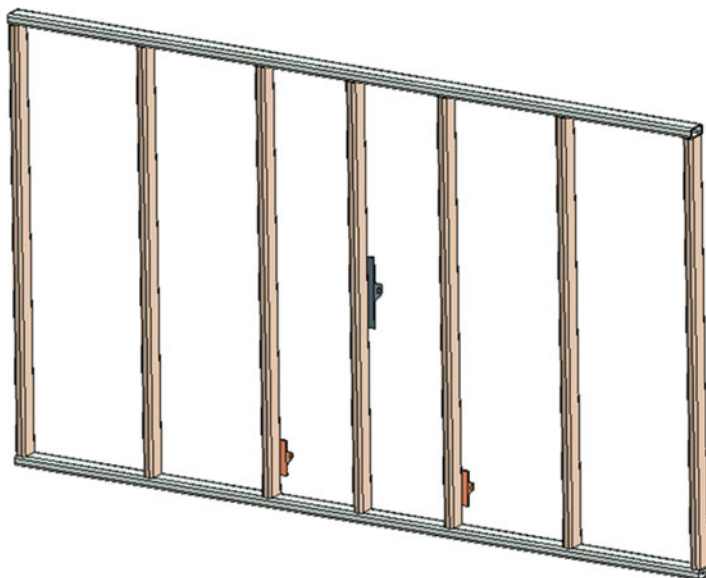


Fig. 4.6 Solar panel frame

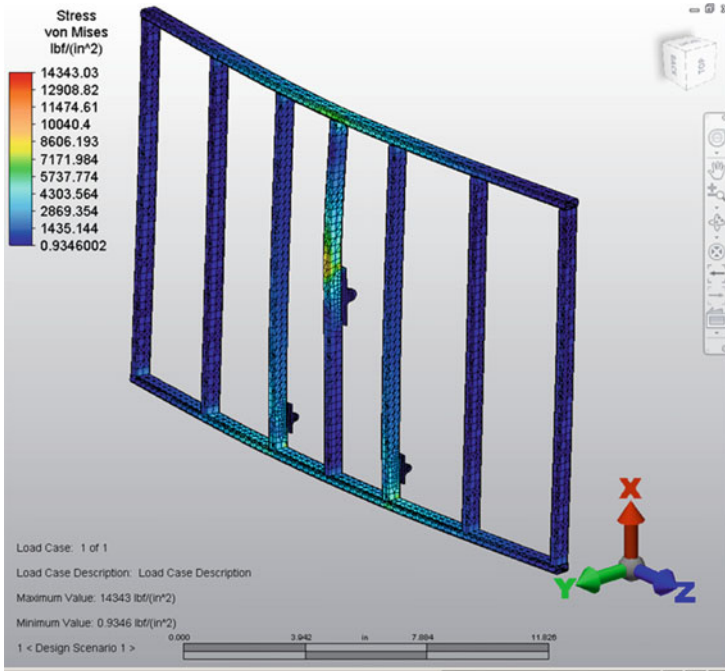


Fig. 4.7 Stress profile in panel frame

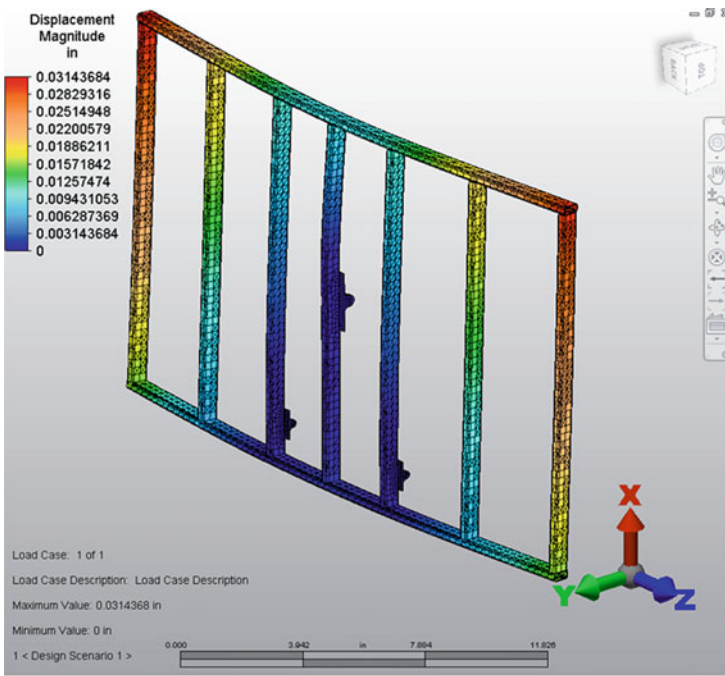


Fig. 4.8 Deflection profile in panel frame

Fig. 4.9 Lateral channel beam

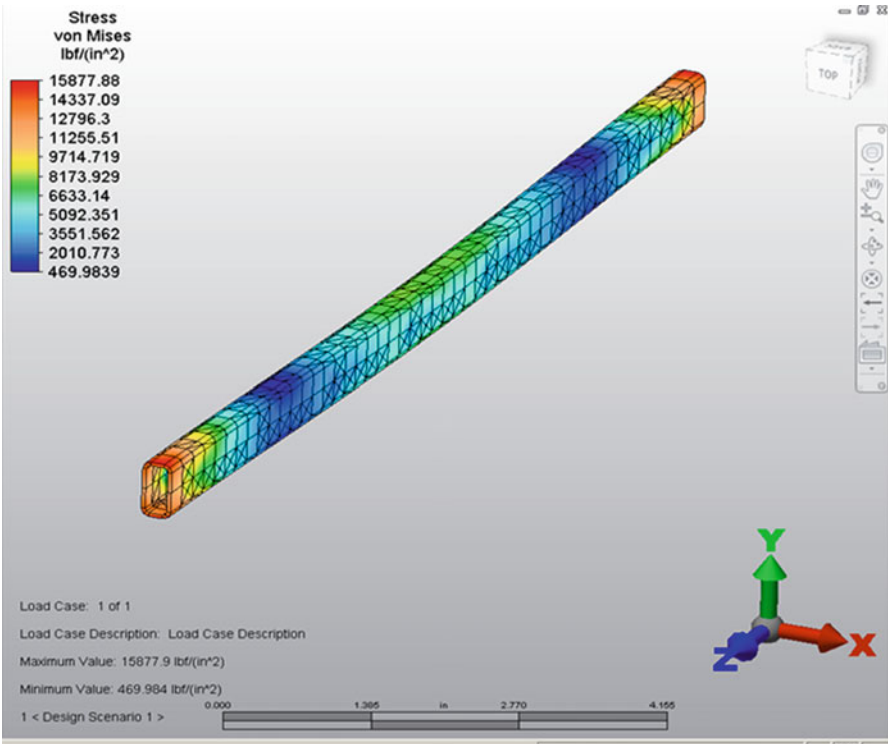
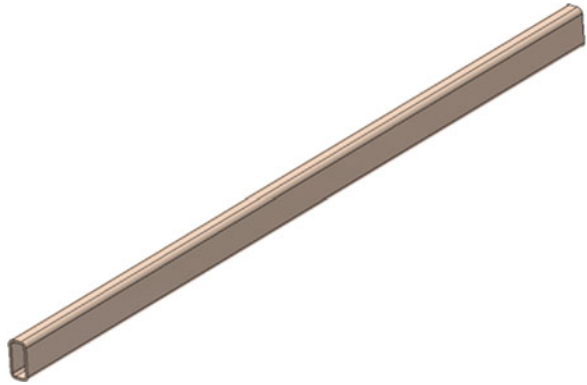


Fig. 4.10 Stress profile in lateral channel beam

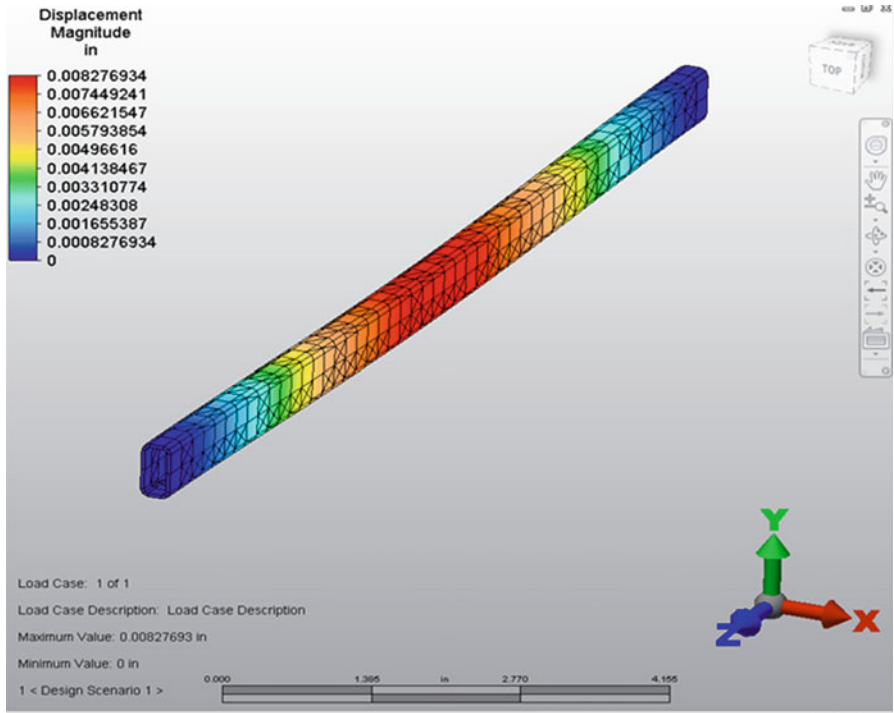
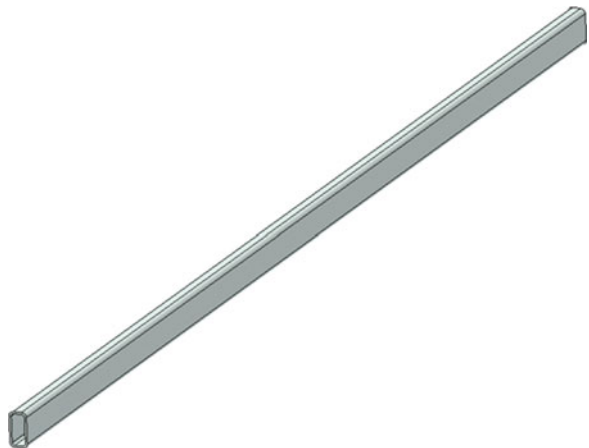


Fig. 4.11 Deflection profile in lateral channel beam

Fig. 4.12 Longitudinal channel beam



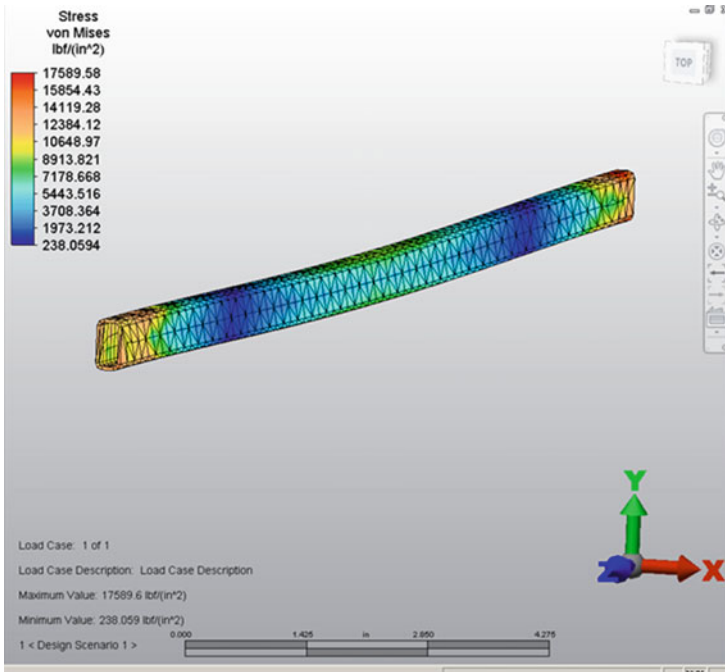


Fig. 4.13 Stress profile in longitudinal channel beam

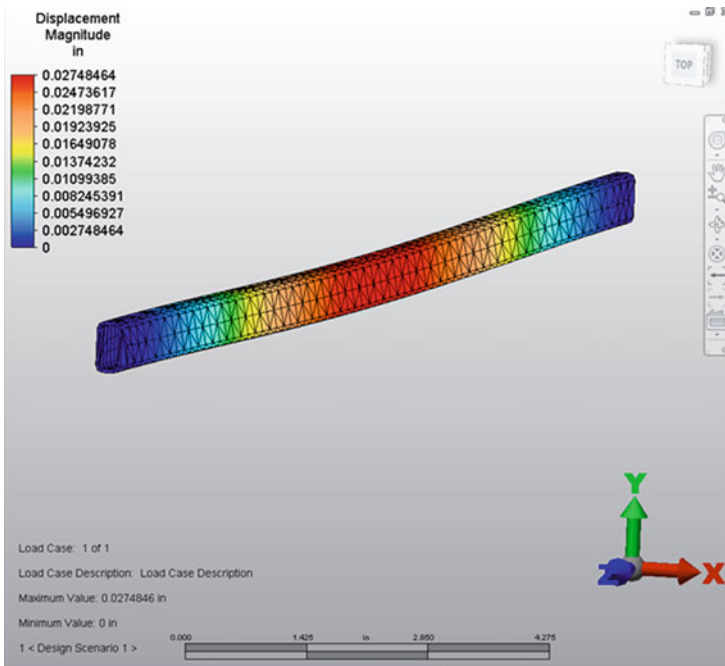


Fig. 4.14 Deflection profile in longitudinal channel beam

Fig. 4.15 Orientation adaptor

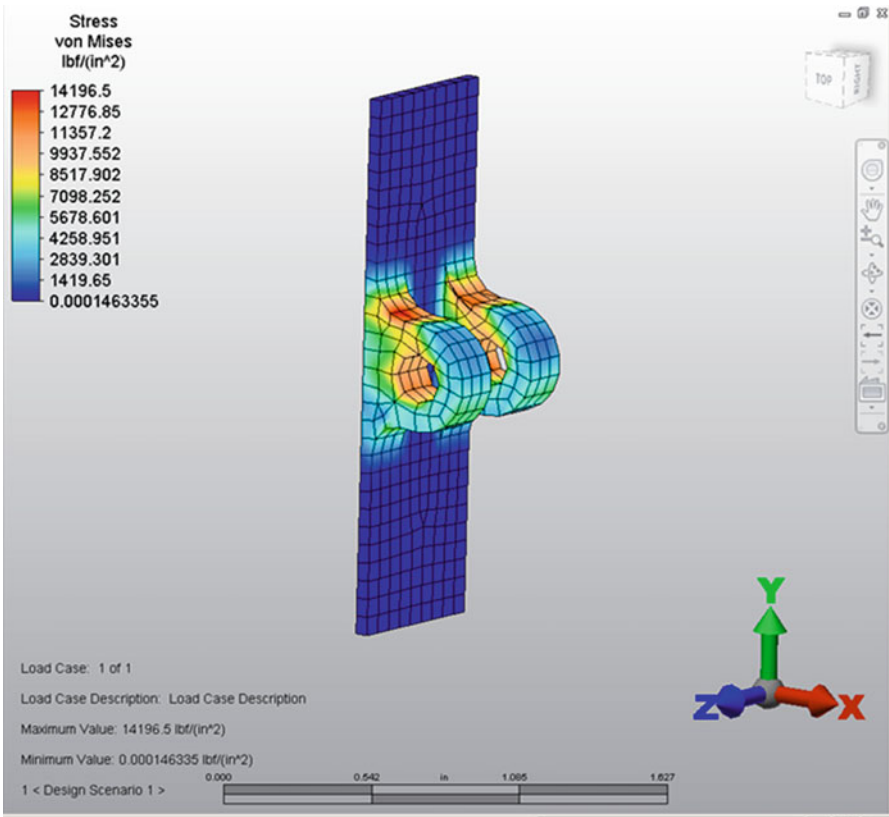
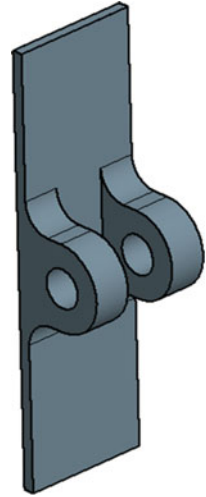


Fig. 4.16 Stress profile in orientation adaptor

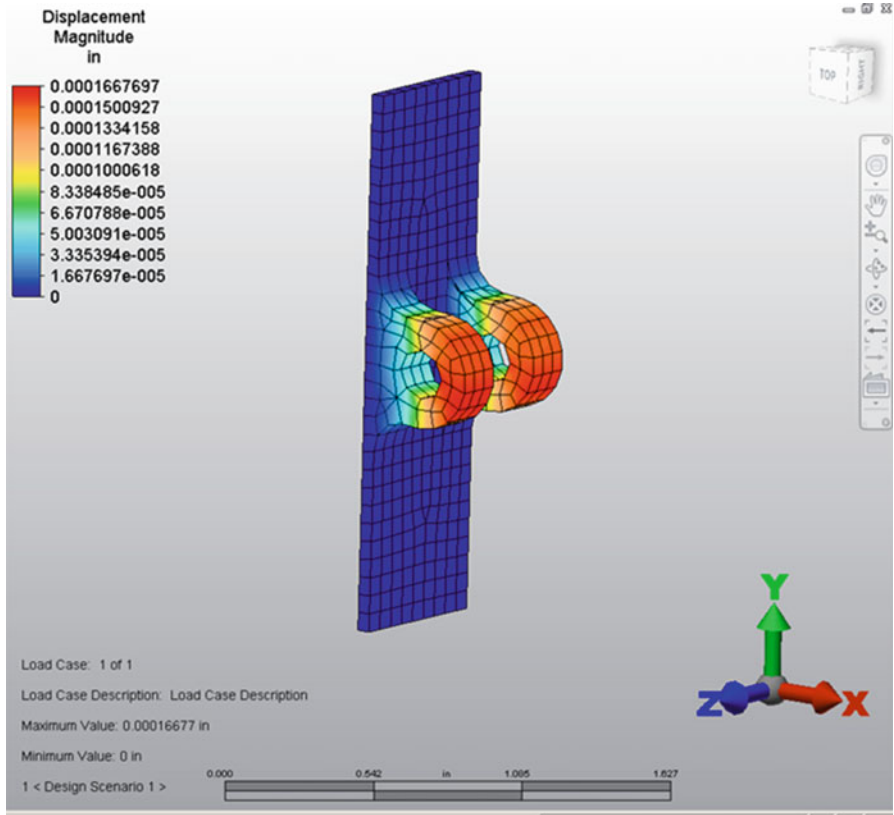
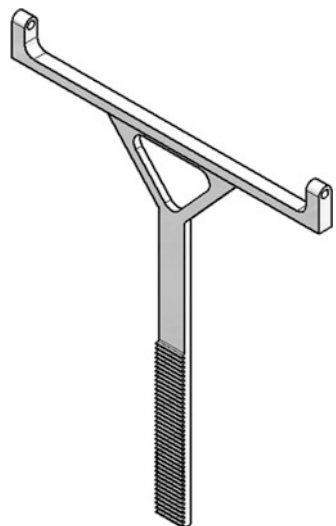


Fig. 4.17 Deflection profile in orientation adaptor

Fig. 4.18 Orientation rack



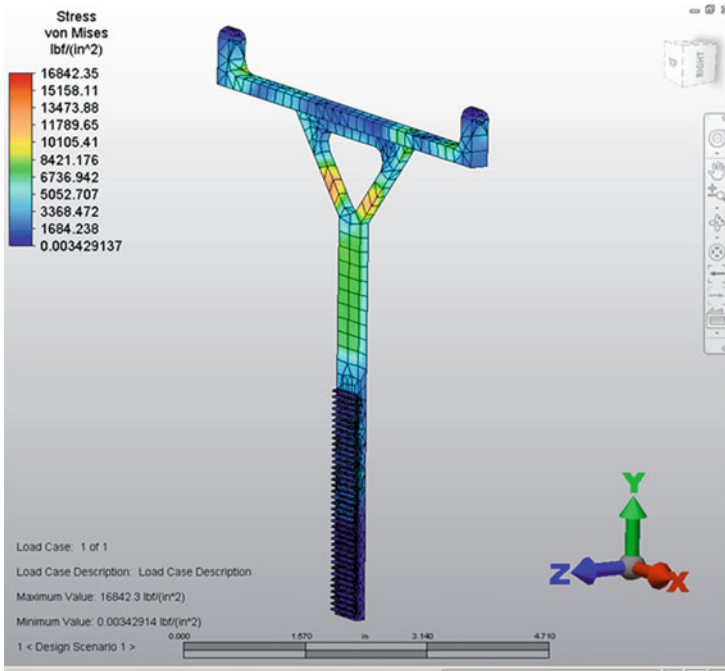


Fig. 4.19 Stress profile in orientation rack

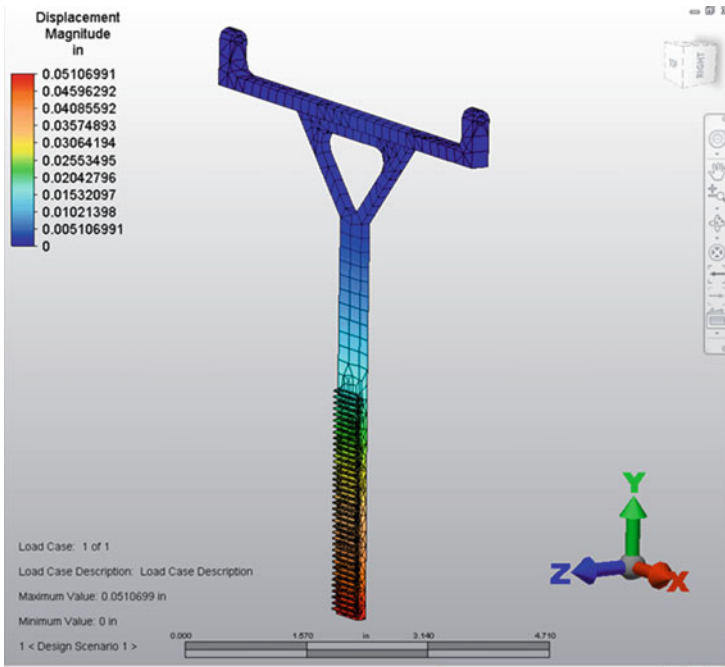


Fig. 4.20 Deflection profile in orientation rack

Fig. 4.21 Orientation base

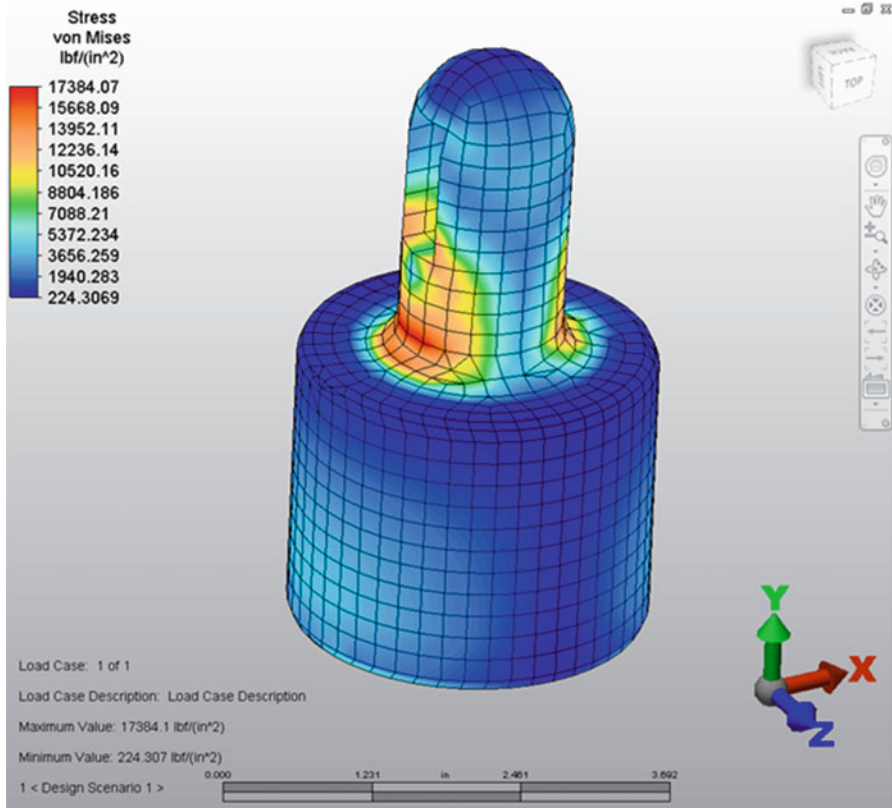
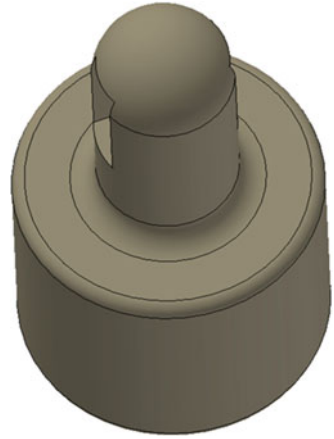


Fig. 4.22 Stress profile in orientation base

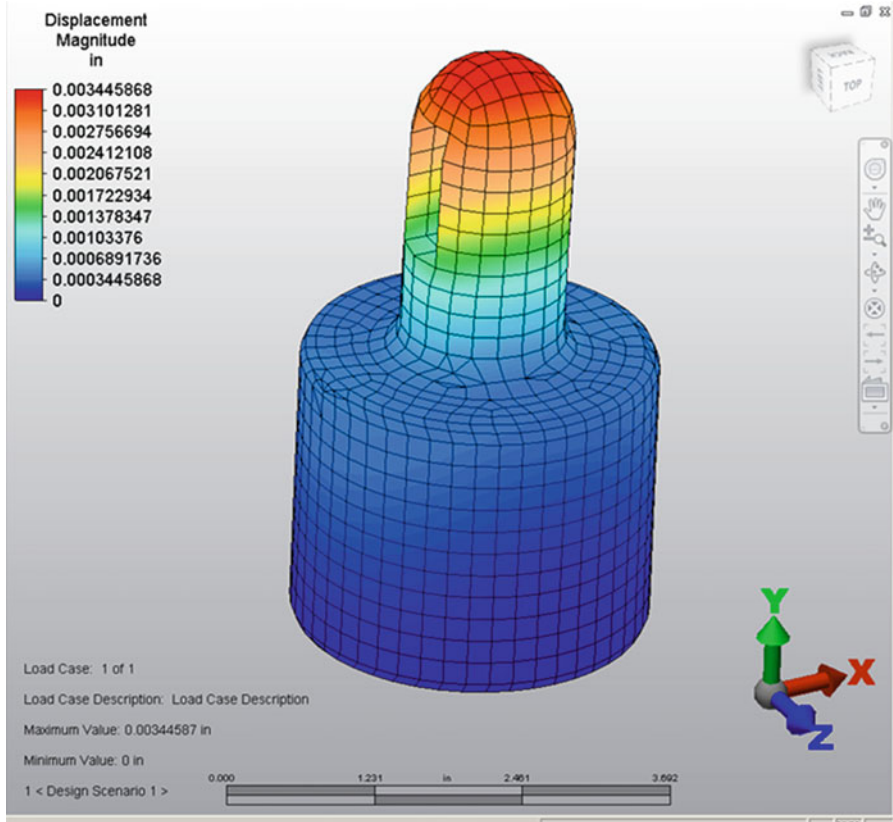
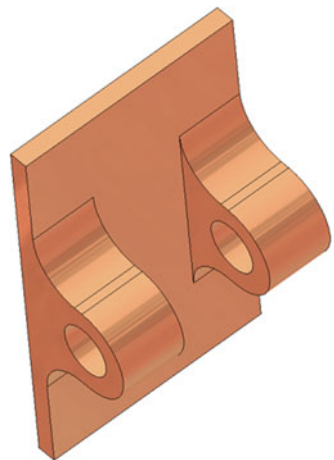


Fig. 4.23 Deflection profile in orientation base

Fig. 4.24 Orientation driver support



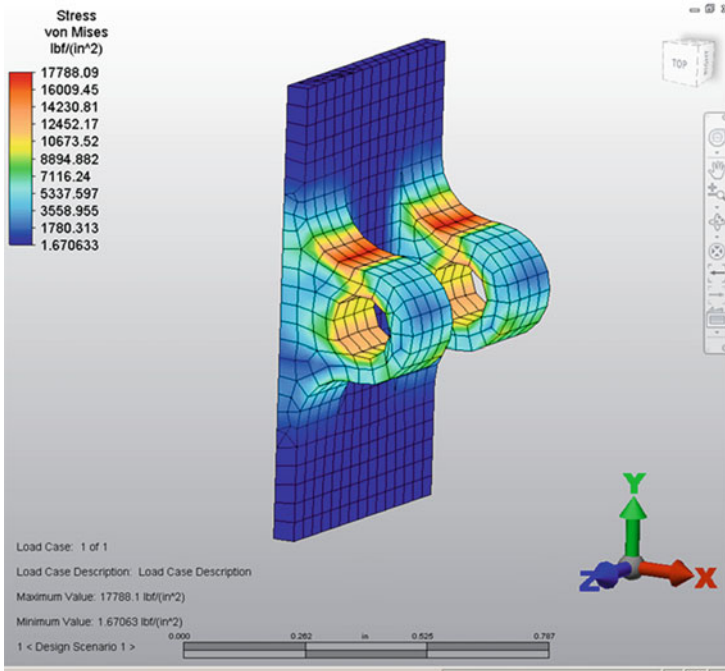


Fig. 4.25 Stress profile in orientation driver support

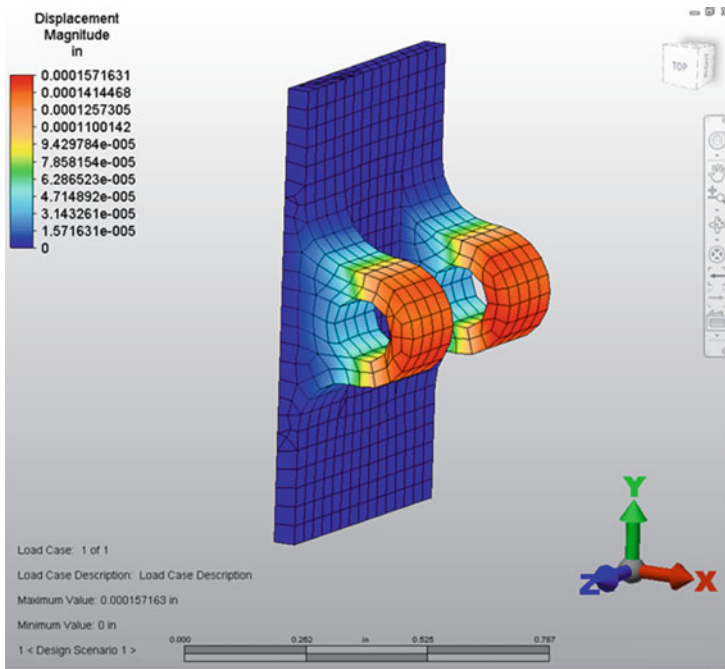


Fig. 4.26 Deflection profile in orientation driver support

Fig. 4.27 Orientation link

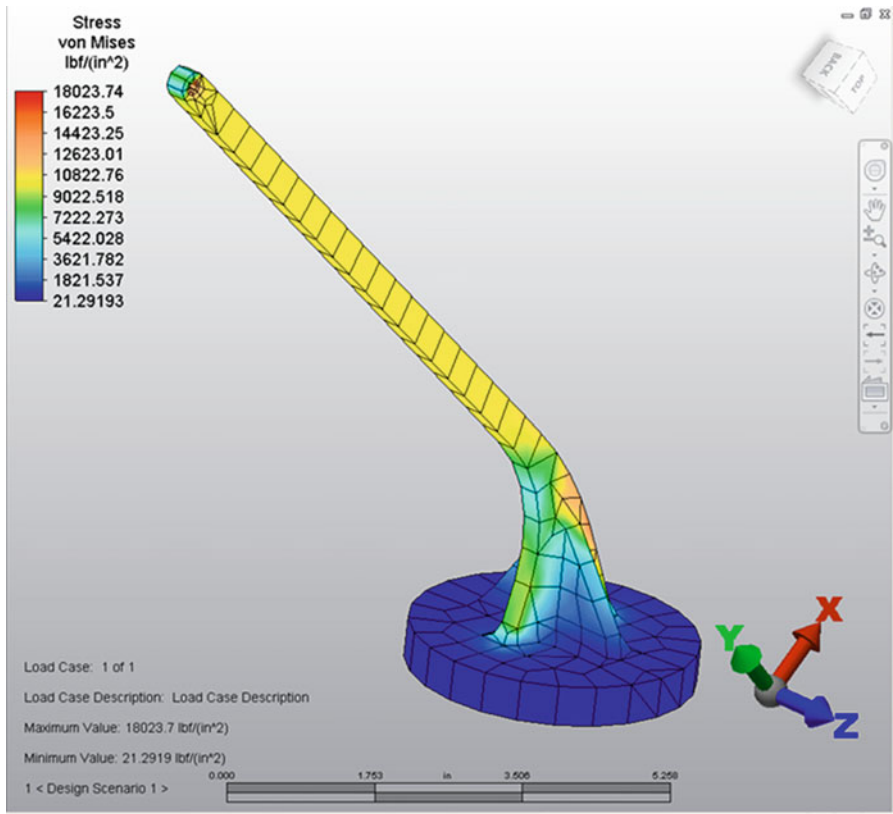
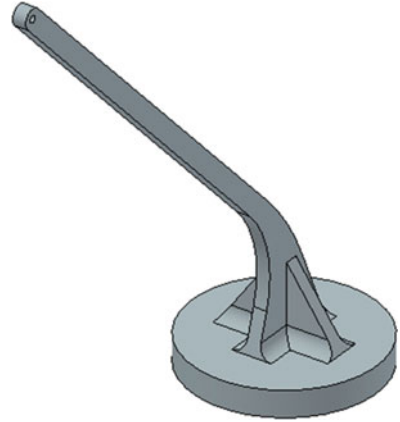


Fig. 4.28 Stress profile in orientation link

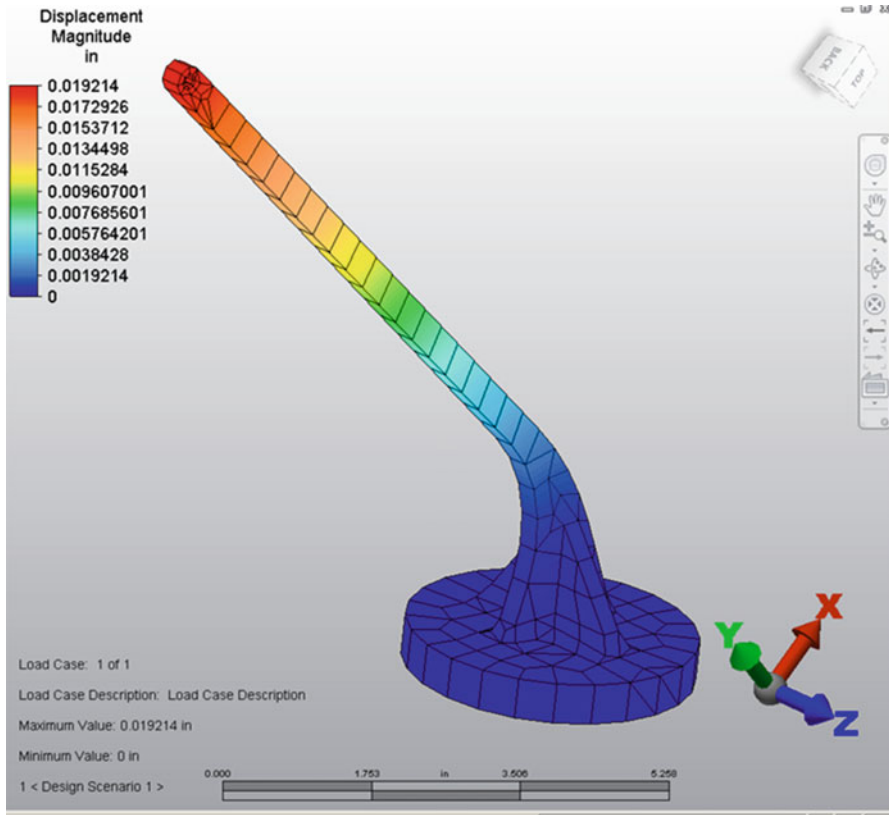


Fig. 4.29 Deflection profile in orientation link

The computer-aided simulation and analysis in Figs. 4.10 and 4.11 indicate the stress and deflection profiles of lateral channel beam in newly designed solar panel system. The analytic results state that the maximum stress of 15,877.88 psi in this lateral channel beam is less than the material yield strength of 36,300 psi and maximum deflection of 0.00828 in. is within material allowable deformation limit.

The computer-aided simulation and analysis in Figs. 4.13 and 4.14 display the stress and deflection profiles of longitudinal channel beam in newly designed solar panel system. The analytic results exhibit that the maximum stress of 17,589.58 psi in this longitudinal channel beam is less than the material yield strength of 36,300 psi and maximum deflection of 0.02748 in. is within material allowable deformation limit.

The computer-aided simulation and analysis in Figs. 4.16 and 4.17 present the stress and deflection profiles of orientation adaptor in newly designed solar panel system. The analytic results demonstrate that the maximum stress of 14,196.50 psi in this orientation adaptor is less than the material yield strength of 36,300 psi and maximum deflection of 0.00017 in. is within material allowable deformation limit.

The computer-aided simulation and analysis in Figs. 4.19 and 4.20 indicate the stress and deflection profiles of orientation rack in newly designed solar panel system. The analytic results state that the maximum stress of 16,842.35 psi in this orientation rack is less than the material yield strength of 36,300 psi and maximum deflection of 0.0511 in. is within material allowable deformation limit.

The computer-aided simulation and analysis in Figs. 4.22 and 4.23 display the stress and deflection profiles of orientation base in newly designed solar panel system. The analytic results exhibit that the maximum stress of 17,384.07 psi in this orientation base is less than the material yield strength of 36,300 psi and maximum deflection of 0.00345 in. is within material allowable deformation limit.

The computer-aided simulation and analysis in Figs. 4.25 and 4.26 present the stress and deflection profiles of orientation driver support in newly designed solar panel system. The analytic results exhibit that the maximum stress of 17,788.09 psi in this orientation base is less than the material yield strength of 36,300 psi and maximum deflection of 0.00016 in. is within material allowable deformation limit.

The computer-aided simulation and analysis in Figs. 4.28 and 4.29 demonstrate the stress and deflection profiles of orientation link in newly designed solar panel system. The analytic results indicate that the maximum stress of 18,023.74 psi in this orientation link is less than the material yield strength of 36,300 psi and maximum deflection of 0.01921 in. is within material allowable deformation limit.

Based on computer-aided analysis, shown in Figs. 4.3, 4.4, 4.5, 4.6, 4.7, 4.8, 4.9, 4.10, 4.11, 4.12, 4.13, 4.14, 4.15, 4.16, 4.17, 4.18, 4.19, 4.20, 4.21, 4.22, 4.23, 4.24, 4.25, 4.26, 4.27, 4.28, and 4.29, the maximum stresses generated in all important components including panel frame, lateral channel beam, longitudinal channel beam, orientation adaptor, orientation rack, orientation base, orientation driver support, and orientation link are all less than the material yield stress and the relevant maximum deflections of these components are all within allowable deformation limits of the materials. The above computational simulations have shown good performance of this newly developed solar tracking system.

4.3 Experiment on Solar Panel Tracking System

New solar panel tracking system has been prototyped and tested to compare and verify the computer-aided simulation results. Table 4.1 demonstrates the experimental results of maximum stress and maximum deflection of solar panel in this new solar panel tracking system.

The prototype experimental results of solar panel in Table 4.1 verify the proper function of this new solar panel system because the average maximum stress 2,267.160 psi and average maximum deflection 0.00519 in. are approximately equal to the results of maximum stress 2,267.076 psi and maximum deflection 0.00507 in. that are represented, respectively, in Figs. 4.4 and 4.5 by computer-aided simulation.

Table 4.2 expresses the experimental results of maximum stress and maximum deflection of solar panel frame in this new solar panel tracking system.

Table 4.1 Experimental results of maximum stress and maximum deflection of solar panel in this new solar panel tracking system

Number of experiment	Maximum stress (psi)	Maximum deflection (in.)
1	2,267.12	0.00505
2	2,267.09	0.00509
3	2,267.15	0.00508
4	2,267.06	0.00511
5	2,267.11	0.00515
6	2,267.15	0.00516
7	2,267.18	0.00524
8	2,267.19	0.00518
9	2,267.17	0.00519
10	2,267.15	0.00527
11	2,267.18	0.00525
12	2,267.21	0.00524
13	2,267.24	0.00522
14	2,267.22	0.00529
15	2,267.18	0.00527
16	2,267.14	0.00526
17	2,267.19	0.00529
18	2,267.18	0.00518
19	2,267.14	0.00519
20	2,267.17	0.00517
Average	2,267.16	0.00519

Table 4.2 Experimental results of maximum stress and maximum deflection of solar panel frame in this new solar panel tracking system

Number of experiment	Maximum stress (psi)	Maximum deflection (in.)
1	14,343.12	0.03124
2	14,343.11	0.03118
3	14,343.08	0.03119
4	14,343.09	0.03129
5	14,343.02	0.03124
6	14,343.15	0.03115
7	14,343.16	0.03148
8	14,343.18	0.03138
9	14,343.19	0.03131
10	14,343.14	0.03124
11	14,343.12	0.03122
12	14,343.01	0.03121
13	14,343.08	0.03118
14	14,343.17	0.03119
15	14,343.24	0.03117
16	14,343.29	0.03124
17	14,343.22	0.03148
18	14,343.24	0.03129
19	14,343.18	0.03125
20	14,343.16	0.03124
Average	14,343.15	0.03126

Table 4.3 Experimental results of maximum stress and maximum deflection of lateral channel beam in this new solar panel tracking system

Number of experiment	Maximum stress (psi)	Maximum deflection (in.)
1	15,877.78	0.00835
2	15,877.84	0.00838
3	15,877.69	0.00837
4	15,877.71	0.00836
5	15,877.68	0.00848
6	15,877.55	0.00846
7	15,877.68	0.00844
8	15,877.65	0.00849
9	15,877.59	0.00845
10	15,877.57	0.00842
11	15,877.66	0.00838
12	15,877.69	0.00847
13	15,877.68	0.00848
14	15,877.78	0.00837
15	15,877.77	0.00844
16	15,877.72	0.00845
17	15,877.67	0.00842
18	15,877.65	0.00848
19	15,877.68	0.00838
20	15,877.71	0.00841
Average	15,877.69	0.00842

The prototype experimental results of solar panel frame in Table 4.2 prove the normal function of solar panel frame as the average maximum stress 14,343.15 psi and average maximum deflection 0.03126 in. are almost same as the results of maximum stress 14,343.03 psi and maximum deflection 0.03143 in. that are indicated, respectively, in Figs. 4.7 and 4.8 by computer-aided simulation.

Table 4.3 records the experimental results of maximum stress and maximum deflection of lateral channel beam in this new solar panel tracking system.

The prototype experimental results of lateral channel beam in Table 4.3 confirm the appropriate function of lateral channel beam since the average maximum stress 15,877.69 psi and average maximum deflection 0.00842 in. are approximately same as the results of maximum stress 15,877.88 psi and maximum deflection 0.00827 in. that are laid out, respectively, in Figs. 4.10 and 4.11 by computer-aided simulation.

Table 4.4 states the experimental results of maximum stress and maximum deflection of longitudinal channel beam in this new solar panel tracking system.

The prototype experimental results of longitudinal channel beam in Table 4.4 verify proper function of this longitudinal channel beam because the average maximum stress 17,589.44 psi and average maximum deflection 0.02761 in. are very close to the results of maximum stress 17,589.58 psi and maximum deflection 0.02748 in. that are shown, respectively, in Figs. 4.13 and 4.14 by computer-aided simulation.

Table 4.4 Experimental results of maximum stress and maximum deflection of longitudinal channel beam in this new solar panel tracking system

Number of experiment	Maximum stress (psi)	Maximum deflection (in.)
1	17,589.48	0.02759
2	17,589.38	0.02754
3	17,589.39	0.02745
4	17,589.44	0.02759
5	17,589.47	0.02768
6	17,589.54	0.02766
7	17,589.49	0.02767
8	17,589.45	0.02765
9	17,589.42	0.02757
10	17,589.38	0.02759
11	17,589.47	0.02768
12	17,589.42	0.02769
13	17,589.48	0.02767
14	17,589.44	0.02768
15	17,589.45	0.02755
16	17,589.38	0.02763
17	17,589.39	0.02765
18	17,589.41	0.02761
19	17,589.42	0.02755
20	17,589.45	0.02759
Average	17,589.44	0.02761

Table 4.5 Experimental results of maximum stress and maximum deflection of orientation adaptor in this new solar panel tracking system

Number of experiment	Maximum stress (psi)	Maximum deflection (in.)
1	14,196.45	0.00019
2	14,196.51	0.00016
3	14,196.42	0.00012
4	14,196.41	0.00014
5	14,196.48	0.00011
6	14,196.35	0.00012
7	14,196.38	0.00011
8	14,196.37	0.00013
9	14,196.31	0.00012
10	14,196.33	0.00011
11	14,196.38	0.00010
12	14,196.41	0.00008
13	14,196.42	0.00009
14	14,196.36	0.00011
15	14,196.35	0.00008
16	14,196.32	0.00007
17	14,196.31	0.00011
18	14,196.33	0.00010
19	14,196.35	0.00012
20	14,196.36	0.00010
Average	14,196.38	0.00011

Table 4.6 Experimental results of maximum stress and maximum deflection of orientation rack in this new solar panel tracking system

Number of experiment	Maximum stress (psi)	Maximum deflection (in.)
1	16,842.25	0.05109
2	16,842.24	0.05115
3	16,842.31	0.05114
4	16,842.21	0.05118
5	16,842.23	0.05117
6	16,842.22	0.05119
7	16,842.21	0.05117
8	16,842.24	0.05115
9	16,842.18	0.05124
10	16,842.19	0.05118
11	16,842.20	0.05115
12	16,842.24	0.05117
13	16,842.21	0.05118
14	16,842.19	0.05119
15	16,842.21	0.05124
16	16,842.18	0.05121
17	16,842.22	0.05122
18	16,842.24	0.05117
19	16,842.18	0.05118
20	16,842.24	0.05116
Average	16,842.22	0.05118

Table 4.5 presents the experimental results of maximum stress and maximum deflection of orientation adaptor in this new solar panel tracking system.

The prototype experimental results of orientation adaptor in Table 4.5 prove the normal function of orientation adaptor as the average maximum stress 14,196.38 psi and average maximum deflection 0.00011 in. are similar to the results of maximum stress 14,196.50 psi and maximum deflection 0.00017 in. that are presented, respectively, in Figs. 4.16 and 4.17 by computer-aided simulation.

Table 4.6 expresses the experimental results of maximum stress and maximum deflection of orientation rack in this new solar panel tracking system.

The prototype experimental results of orientation rack in Table 4.6 confirm the appropriate function of orientation rack since the average maximum stress 16,842.22 psi and average maximum deflection 0.05118 in. are almost equal to the results of maximum stress 16,842.35 psi and maximum deflection 0.05107 in. that are indicated, respectively, in Figs. 4.19 and 4.20 by computer-aided simulation.

Table 4.7 conveys the experimental results of maximum stress and maximum deflection of orientation base in this new solar panel tracking system.

The prototype experimental results of orientation base in Table 4.7 prove the normal function of orientation base as the average maximum stress 17,384.20 psi and average maximum deflection 0.00331 in. are closely equal to the results of

Table 4.7 Experimental results of maximum stress and maximum deflection of orientation base in this new solar panel tracking system

Number of experiment	Maximum stress (psi)	Maximum deflection (in.)
1	17,384.15	0.00338
2	17,384.17	0.00333
3	17,384.06	0.00348
4	17,384.18	0.00341
5	17,384.24	0.00337
6	17,384.22	0.00324
7	17,384.25	0.00329
8	17,384.21	0.00327
9	17,384.17	0.00325
10	17,384.18	0.00332
11	17,384.19	0.00327
12	17,384.18	0.00325
13	17,384.22	0.00327
14	17,384.24	0.00330
15	17,384.25	0.00327
16	17,384.26	0.00329
17	17,384.24	0.00324
18	17,384.19	0.00326
19	17,384.18	0.00331
20	17,384.17	0.00330
Average	17,384.20	0.00331

Table 4.8 Experimental results of maximum stress and maximum deflection of orientation driver support in this new solar panel tracking system

Number of experiment	Maximum stress (psi)	Maximum deflection (in.)
1	17,788.15	0.00017
2	17,788.08	0.00019
3	17,788.17	0.00018
4	17,788.18	0.00024
5	17,788.19	0.00025
6	17,788.16	0.00026
7	17,788.08	0.00023
8	17,788.12	0.00025
9	17,788.19	0.00029
10	17,788.18	0.00027
11	17,788.24	0.00029
12	17,788.24	0.00027
13	17,788.21	0.00024
14	17,788.27	0.00026
15	17,788.26	0.00025
16	17,788.27	0.00024
17	17,788.24	0.00029
18	17,788.22	0.00027
19	17,788.24	0.00026
20	17,788.21	0.00024
Average	17,788.20	0.00025

Table 4.9 Experimental results of maximum stress and maximum deflection of orientation link in this new solar panel tracking system

Number of experiment	Maximum stress (psi)	Maximum deflection (in.)
1	18,023.68	0.01915
2	18,023.66	0.01916
3	18,023.62	0.01918
4	18,023.54	0.01911
5	18,023.59	0.01912
6	18,023.78	0.01911
7	18,023.67	0.01915
8	18,023.62	0.01910
9	18,023.60	0.01911
10	18,023.61	0.01912
11	18,023.54	0.01908
12	18,023.55	0.01910
13	18,023.57	0.01911
14	18,023.56	0.01912
15	18,023.57	0.01914
16	18,023.55	0.01915
17	18,023.59	0.01911
18	18,023.61	0.01912
19	18,023.62	0.01910
20	18,023.63	0.01914
Average	18,023.61	0.01912

maximum stress 17,384.07 psi and maximum deflection 0.00335 in. that are recorded, respectively, in Figs. 4.22 and 4.23 by computer-aided simulation.

Table 4.8 lays out the experimental results of maximum stress and maximum deflection of orientation driver support in this new solar panel tracking system.

The prototype experimental results of orientation driver support in Table 4.8 verify the proper function of orientation driver support because the average maximum stress 17,788.20 psi and average maximum deflection 0.00025 in. are almost same as the results of maximum stress 17,788.09 psi and maximum deflection 0.00016 in. that are displayed, respectively, in Figs. 4.25 and 4.26 by computer-aided simulation.

Table 4.9 shows the experimental results of maximum stress and maximum deflection of orientation link in this new solar panel tracking system.

The prototype experimental results of orientation link in Table 4.9 confirm the appropriate function of orientation link since the average maximum stress 18,023.61 psi and average maximum deflection 0.01912 in. are approximately equal to the results of maximum stress 18,023.74 psi and maximum deflection 0.01921 in. that are exhibited, respectively, in Figs. 4.28 and 4.29 by computer-aided simulation.

4.4 Discussion and Future Improvement on Solar Panel Tracking System

Solar power system can transfer the natural sunlight energy to the electrical mechanical energies. It has the major advantages including safe and clean features compared to the traditional energy resources. This chapter introduces the methodologies using computational simulation and prototype testing to determine the important factors affecting the performance of this new solar panel tracking system. Both computational simulation and prototype experiment show its reliable function. Future improvement has been planned to optimize this solar tracking system by computer-aided modeling and analysis to determine the optimal working condition, further reduce system weight to save system cost, and revise the gear train for more quiet operation.